Title
Chronic copper exposure directs microglia towards degenerative expression signatures in wild-type and J20 mouse model of Alzheimer's disease

Authors
Lim, Siok Lam
Rodriguez-Ortiz, Carlos J
Hsu, Heng-Wei
et al.

Publication Date
2020-12-01

DOI
10.1016/j.jtemb.2020.126578

Peer reviewed

HHS Public Access

Author manuscript

J Trace Elem Med Biol. Author manuscript; available in PMC 2021 December 01.

Published in final edited form as:

J Trace Elem Med Biol. 2020 December ; 62: 126578. doi:10.1016/j.jtemb.2020.126578.

Chronic copper exposure directs microglia towards degenerative expression signatures in wild-type and J20 mouse model of Alzheimer's disease

Siok Lam Lim[a], **Carlos J. Rodriguez-Ortiz**[a,#], **Heng-Wei Hsu**[a,#], **Jie Wu**[b], **Joannee Zumkehr**[a], **Jason Kilian**[a], **Janielle Vidal**[a], **Pinar Ayata**[c], **Masashi Kitazawa**[a,*]

[a]Center for Occupational and Environmental Health, Department of Medicine, University of California, Irvine, California, USA

[b]Department of Biological Chemistry, University of California, Irvine, California, USA

[c]Nash Family Department of Neuroscience, Ronald M. Loeb Center for Alzheimer's Disease, Icahn School of Medicine at Mount Sinai, New York, USA

Abstract

BACKGROUND—Copper (Cu) is an essential metal mediating a variety of vital biological reactions with its redox property. Its dyshomeostasis has been associated with accelerated cognitive decline and neurodegenerative disorders, such as Alzheimer's disease (AD). However, underlying neurotoxic mechanisms elicited by dysregulated Cu remain largely elusive. We and others previously demonstrated that exposure to Cu in drinking water significantly exacerbated pathological hallmarks of AD and pro-inflammatory activation of microglia, coupled with impaired phagocytic capacity, in mouse models of AD.

METHODS—In the present study, we extended our investigation to evaluate whether chronic Cu exposure to wild-type (WT) and J20 mouse model of AD perturbs homeostatic dynamics of microglia and contributes to accelerated transformation of microglia towards degenerative phenotypes that are closely associated with neurodegeneration. We further looked for evidence of

[*]**Corresponding author:** Masashi Kitazawa, Ph.D., Associate Professor, Center for Occupational and Environmental Health, Department of Medicine, University of California, Irvine, 100 Theory Dr., Suite 100, Irvine, CA 92617 +1-949-824-1255, kitazawa@uci.edu.

[#]Both authors contributed equally to this manuscript.

Author Statement

Siok Lam Lim: Project administration, Methodology, Validation, Investigation, Data Curation, Formal analysis, Writing - Original Draft, Visualization, Writing - Review & Editing, Funding acquisition

Carlos J. Rodriguez-Ortiz: Methodology, Validation, Investigation, Data Curation, Formal analysis, Writing - Original Draft, Visualization Heng-Wei Hsu: Investigation

Jie Wu: Methodology, Formal analysis, Data Curation Joannee Zumkehr: Investigation Jason Kilian: Investigation Janielle Vidal: Investigation

Pinar Ayata: Methodology, Formal analysis, Visualization, Writing - Review & Editing, Funding acquisition

Masashi Kitazawa: Conceptualization, Supervision, Resources, Methodology, Formal analysis, Visualization, Writing - Review & Editing, Funding acquisition

Conflict of interest statement

The authors declare that they have no competing interests.

alterations in the microglial morphology and spatial memory of the Cu-exposed mice to assess the extent of the Cu toxicity.

RESULTS—We find that chronic Cu exposure to pre-pathological J20 mice upregulates the translation of degenerative genes and represses homeostatic genes within microglia even in the absence amyloid-beta plaques. We also observe similar expression signatures in Cu-exposed WT mice, suggesting that excess Cu exposure alone could lead to perturbed microglial homeostatic phenotypes and contribute to accelerated cognitive decline.

CONCLUSION—Our findings highlight the risk of chronic Cu exposure on cognitive decline and altered microglia activation towards degenerative phenotypes. These changes may represent one of the key mechanisms linking Cu exposure or its dyshomeostasis to an increased risk for AD.

Keywords

Copper; Alzheimer's disease; Microglia; Translating ribosome affinity purification (TRAP); Translatome

1. Introduction

Alzheimer's disease (AD) is the leading cause of dementia with unknown etiology. While aging and genetic predisposition contribute greatly to the increasing risk for AD, exposure to environmental contaminants, diets, and lifestyle are also empirically known to modulate the progression and onset of AD through multifaceted mechanisms [1, 2]. Among these suspected environmental risk factors, accumulating evidence indicates that copper (Cu) dyshomeostasis in the body, most notably by elevated levels of labile or free Cu in blood, correlate strongly with poor cognitive performance, reduced amyloid-beta (Aβ) in cerebrospinal fluid (CSF), and increased CSF tau as well as accelerated conversion from mild cognitive impairment (MCI) stage to clinically diagnosed AD stage [3-9]. This correlation remains true even among non-demented elderly population as excess Cu intake from dietary supplements or elevated serum Cu is consistently associated with hippocampal volume loss and impaired memory function [10-12], further supporting a profound adverse effect of free Cu releases by Cu dyshomeostasis or excessive exposure in the central nervous system (CNS) and as a precursor to dementia. The preponderance of Cu found in solid food is present in organic molecules as the cuprous Cu^{+} form, which is efficiently absorbed by the intestinal microvilli and has essential nutritional value, while that found in drinking water, environment, or dietary supplements is in the inorganic cupric Cu^{2+} form [13-15], whose uptake process in the intestine is less understood. Rapid elevation of Cu in the blood following ingestion of Cu-containing water indicates a possibility of bypassing the proper metabolic process to enter the circulation [16].

Chronic exposure to Cu through drinking water, even at trace amount, has been shown to exacerbate Aβ plaque pathology in animal models [17, 18]. Mechanistically, it has been suggested that altered distribution of Cu [19], amyloid precursor protein (APP) processing [20], Cu-Aβ interaction and oligomerization [21, 22], inflammation [23-26], and loss of endothelial low-density lipoprotein-like receptor protein 1 (LRP1) [27, 28] modulate the development of AD neuropathology and cognitive function. On the contrary, deficiency of

Cu could also be detrimental as it leads to aggravated glial responses and impaired antioxidative defense in the brain [29, 30].

In the present study, we extended our investigation to evaluate whether chronic Cu exposure through drinking water perturbs homeostatic dynamics of microglia in wild-type (WT) and J20 mouse model of AD and contributes to accelerated transformation of microglia towards degenerative phenotypes that have recently been reported to be associated with neurodegeneration [31]. We find that chronic Cu exposure shifts microglia towards degenerative phenotypes at translational levels, even in the pre-pathological stage of J20 mice as well as in its WT counterpart. Cu-exposed mice display impaired cognition, which correlates with appearance of inflammatory phenotypes of microglia based on translatomic analysis. These findings highlight the critical role of microglia and their contribution to the AD pathology as shown in recent emerging evidence [31-34]. Taken together, our findings provide evidence that excess Cu exposure may pose a risk to accelerate cognitive decline and progression of AD by mechanistically perturbing microglial homeostasis and driving microglia towards more neurodegenerative phenotypes.

2. Materials and methods

2.1. Animals

Hemizygous *PDGF-hAPP*$_{Sw,Ind}$ J20 mice (stock number: 34836-JAX), strain-matched wild-type (WT) C57BL/6J mice, *Cx3cr1*^{CreER} mice [35] (stock number: 021160), and *Rosa26*^{fsTRAP} mice [36] (stock number: 022367) were purchased from Jackson Laboratory. *Cx3cr1*^{CreER} mice express tamoxifen-inducible Cre recombinase (Cre-ERT2), and upon tamoxifen induction, more than 99% of microglia in *Cx3cr1*^{CreER} mice expressed Cre-ERT2, which was visualized by the expression of enhanced yellow fluorescent protein (EYFP) driven by an internal ribosome entry site (IRES) following the *Cre-ERT2* gene [35, 37]. In addition, this particular strain of Cx3cr1^{CreER} mice has been reported to possess tight regulation of Cre recombinase activation with the highest selectivity when compared with other strains, and the presence of EYFP in microglia does not interfere with microglia-specific translating ribosome affinity purification (TRAP) procedure described below [37].

To obtain microglia-specific TRAP mice with or without J20 genotype, *Cx3cr1*$^{CreER/CreER}$;*Rosa26*$^{fsTRAP/fsTRAP}$ mice were crossed with J20 mice to generate *J20;Cx3cr1*$^{CreER/+}$;*Rosa26*$^{fsTRAP/+}$ (herein referred to as J20/TRAP/Cx3cr1 or JTCx) and *WT;Cx3cr1*$^{CreER/+}$;*Rosa26*$^{fsTRAP/+}$ (herein referred to as WT/TRAP/Cx3cr1 or WTCx) mice, respectively (Fig. 1A). Age-matched J20 and WT mice were also used for behavioral studies and immunohistochemical staining. All mice were of C57BL/6J background, and both genders were used in this study.

Mice were exposed to 1.3 ppm Cu-containing Milli-Q water (Cu) or Milli-Q water (H_2O) for 3 or 5 months, starting at 1 month of age, and were analyzed at 4 or 6-month old when JTCx or J20 mice were at an early stage of pathological development. The applied Cu concentration for the study is the maximum recommended level permitted by the United States Environmental Protection Agency in drinking water (https://www.epa.gov/dwreginfo/lead-and-copper-rule). It is thus an environmentally relevant dose for investigating the

effects of chronic Cu exposure through drinking water. The Cu drinking water was prepared from copper (II) chloride dihydrate ($CUCl_2.2H_2O$) of ≥ 99.99% purity (MilliporeSigma, catalog # 467847). Ultrapure Milli-Q water (MilliporeSigma) was used to dissolve the Cu salt at 1.3 ppm where background equivalent concentration of Cu in the purified water has been reported at 0.19 ppt (https://www.sigmaaldrich.com/technical-documents/articles/biology/water-purification-systems/ultrapure-water-elemental-impurities-pharma.html). Both Cu and control drinking water were given ad libitum, as well as the chow diet. Mice were fed with 2020X Teklad global soy protein-free extruded rodent diet (Envigo) which contains equivalent amount of Cu (15 mg/kg) in diet used in previous studies assessing neurotoxic effects of Cu through drinking water [23, 28].

To activate tamoxifen-inducible Cre/loxP recombination, mice were injected intraperitoneally with either 2 mg/day of tamoxifen (T5648, MilliporeSigma) dissolved in corn oil or 100 μl corn oil (as negative control) for 5 consecutive days, starting at 2 to 4 weeks before the mice were sacrificed, as modified from a recently published method [38]. All animal studies performed were approved by the University of California Institutional Animal Care and Use Committee and were in accordance with Federal guidelines.

2.2. Isolation of microglia using Percoll gradient

The extraction of microglia from adult mice was adapted with modification from published method [35]. Briefly, mice were sacrificed by anesthesia overdose intraperitoneally before perfused with ice-cold phosphate buffered saline (PBS). Half brain was collected and removed of brainstem and cerebellum before placing in chilled PFH (PBS/fetal calf serum/HEPES) solution comprising of Ca^{2+}/Mg^{2+}-free DPBS (Dulbecco's Phosphate-Buffered Saline, Life Technologies) with 5% fetal calf serum and 1 mM 4-(2-hydroxyethyl)-1-piperazineethanesulfonic acid (HEPES, Thermo Fisher Scientific), pH 7.4. Brain tissue was minced with scissors, and incubated in 400 Mandl U Collagenase D (Roche) at 37°C for 30 min for enzymatic digestion, before incubated in 10 mM ethylenediaminetetraacetic acid (EDTA, Thermo Fisher Scientific) for an additional 5 min at 37°C for Collagenase inactivation. Digested tissue was next triturated through an 18G needle before filtered through a 70 μm cell strainer, and centrifuged at 1500 rpm for 5 min to pellet cells. Cell pellet was then resuspended in 38% Percoll solution (MilliporeSigma), before centrifuging at 2000 rpm for 30 min to obtain the interphase that contained microglial cells. Finally, the microglial cell pellet was resuspended in PFH solution for washing and collected by centrifugation at 1500 rpm for 5 min.

2.3. Protein extraction and western blot analysis

Protein lysate was extracted from isolated microglial cells by lysing in T-PER Tissue Protein Extraction Reagent (Thermo Fisher Scientific) complemented with protease and phosphatase inhibitors (MilliporeSigma), followed by centrifugation at 14,000 rpm at 4°C for 20 min. Protein concentration was determined using the Bradford protein assay. Standardized protein mass were separated by sodium dodecyl sulphate-polyacrylamide gel electrophoresis (SDS-PAGE) and transferred to Immobilon-FL polyvinylidene fluoride (PVDF) membrane (EMD Millipore). Membranes were blocked in Odyssey Blocking Buffer (LI-COR Biosciences) for 1 h at room temperature, before immunoblotted overnight with shaking at 4°C with the

following antibodies diluted in Odyssey Blocking Buffer with 0.2% Tween 20 (Thermo Fisher Scientific): Green fluorescent protein (GFP, Rockland Immunochemicals Inc., catalog # 600-101-215, goat polyclonal, 1:200 dilution) and Glyceraldehyde 3-phosphate dehydrogenase (GAPDH, Santa Cruz Biotechnology Inc., catalog # sc-25778, rabbit polyclonal, 1:5000 dilution). Membranes were then washed in Tris-buffered saline with 0.1% Tween 20 (TBST), before incubated with corresponding IRDye secondary antibodies (LI-COR Biosciences, raised in donkey or goat, 1:20000 dilution) diluted in TBST/SDS and 5% fat-free milk for 1 h at room temperature. Membranes were washed in TBST thereafter and scanned using Odyssey Imaging System (LI-COR Biosciences). Band intensities were quantified with Image Studio software (version 5.2, LI-COR Biosciences) and normalized to that of GAPDH which serves as protein loading control.

2.4. Translating ribosome affinity purification (TRAP)

Ribosome-associated mRNA from microglia was extracted using TRAP technique adapted from previously described [37, 39]. Briefly, two hippocampi per euthanized mouse were immediately homogenized with a motor-driven Teflon-glass homogenizer (Fisher Scientific) in ice-cold tissue lysis buffer comprised of 20 mM HEPES (pH 7.3, Affymetrix), 150 mM potassium chloride (KCl, Ambion), 10 mM magnesium chloride ($MgCl_2$, Ambion), EDTA-free protease inhibitor cocktail (Roche), 0.5 mM dithiothreitol (DTT, MilliporeSigma), 100 μg/ml cycloheximide (MilliporeSigma), 10 μl/ml RNasin (Promega) and 10 μl/ml Superasin (Applied Biosystems). Homogenates were centrifuged at 4°C for 10 min at 2,000g to pellet large cell debris. Nonylphenyl-polyethylene glycol (NP-40, AG Scientific) and 1,2-diheptanoyl-sn-glycero-3-phosphocholine (DHPC, Avanti Polar Lipids) were added to the supernatant at final concentrations of 1% and 30 mM, respectively. After incubation on ice for 5 min, the lysate was centrifuged at 4°C for 10 min at 20,000g to pellet insoluble material. GFP antibodies (clone names: Htz-GFP-19C8 and Htz-GFP-19F7, Memorial Sloan-Kettering Cancer Center, mouse monoclonal) and biotinylated Protein L (GenScript)-coated Streptavidin MyOne T1 Dynabeads (Invitrogen) were added to the supernatant, and the mixture was incubated at 4°C with end-over-end mixing in a tube rotator overnight. Polysome bound-beads were collected on a magnetic rack and washed four times with high-salt buffer (20 mM HEPES (pH 7.3), 350 mM KCl, 10 mM $MgCl_2$, 1% NP-40, 0.5 mM DTT, and 100 μg/mL cycloheximide). An aliquot of the unbound (UB) fraction was saved for enrichment assessment later. Microglia-specific RNA (TRAP) sample was purified directly from beads using RNeasy Micro Kit (Qiagen) following the manufacturer's instructions.

2.5. Quantitative polymerase chain reaction (qPCR)

RNA integrity was assessed using RNA Pico chip on Bioanalyzer 2100 (Agilent). Only samples with RNA integrity number (RIN) ≥ 9 were used for subsequent experiments. Total RNA was reversed-transcribed to cDNA using iScript cDNA Synthesis kit (Bio-Rad Laboratories). cDNA was loaded for qPCR on Bio-Rad Laboratories CFX Manager 3.1 using TaqMan Universal PCR Master Mix (Life Technologies) following the manufacturer's recommendations. TaqMan probes (Life Technologies) used were *Cx3cr1* (Mm02620111_s1), *Aldh1a1* (Mm00657317_m1), *Rbfox3/NeuN* (Mm01248771_m1), and *Gapdh* (Mm99999915_g1). Relative fold change of mRNA levels were calculated by the 2-

$^{\Delta\Delta Ct}$ method (Livak and Schmittgen, 2001) using *Gapdh* as the reference gene and genes expressed by associated TRAP/UB samples as the calibrators.

2.6. RNA sequencing (RNA-seq)

TRAP and UB sample pairs with RIN ≥ 9 and verified as microglia-enriched by qPCR were loaded at 500 pg for cDNA synthesis using Ovation® RNA-Seq System V2 (NuGen). External controls - ERCC spike-in control mixes (Life Technologies) - were added to each reaction according to the manufacturer's instructions. cDNA was sheared to 300 bp using S220 Focused-ultrasonicator (Covaris). Sheared cDNA was checked for sizing using Bioanalyzer High Sensitivity DNA chip (Agilent). Illumina ready libraries were constructed using Ovation® Ultralow System V2 1-96 kit (NuGen). The libraries were quantified by Qubit dsDNA High Sensitivity Assay kit (Thermo Fisher Scientific), and the size was analyzed by Bioanalyzer High Sensitivity DNA chip. The libraries were normalized to 2 ng/μl and multiplexed together. The pooled libraries were again quantified by Qubit, and the size in bp was measured by Bioanalyzer High Sensitivity DNA chip. The final quantification was performed by KAPA Library Quantification Kit Illumina (Kapa Biosystems). Multiplexed libraries were loaded directly on HiSeq 4000 System (Illumina) with paired end 100 bp reads.

2.7. Bioinformatic analysis of RNA-seq data

Raw reads were generated using Illumina software bcl2fastq. Raw reads were then QCed for quality (FASTQC), trimmed (Trimmomatic) and aligned to the mouse reference genome (mm10) with a splice aware short read aligner (TopHat2). Expression level was quantified using raw counts (featureCounts) and Fragments Per Kilobase of transcript per Million mapped reads (FPKM) values for known genes (Cufflinks). Principal component analysis (PCA) and differential gene expression analysis (differentially expressed genes, DEGs) were done using R package DESeq2. ERCC control analysis was done using R package erccdashboard.

For all comparisons, a cutoff of $p < 0.05$, fold-change > 2, and mean expression > 20 was applied (DESeq2; n = 3-4 mice per group). Additionally, for the TRAP samples, an enrichment cutoff of $p < 0.05$ and fold-change > 2 over their respective UB fraction was applied. All of the volcano, MA, scatter plots, heatmaps, and histograms for bulk sequencing were made using R (v3.1.1; https://www.R-project.org). Gene Ontology (GO) term enrichment analysis was performed using Enrichr. Selected and significantly enriched ($p < 0.05$ with BH correction) GO annotations for biological processes are represented in bar graphs. Ingenuity Pathway Analysis (IPA, Qiagen) was used to predict diseases and biological functions that were triggered by translatomes that were significantly altered by AD pathology or Cu exposure. Dataset were filtered with cutoff of fold-change > 2 and FDR < 0.1.

2.8. Inmnmohistochemical analysis

Littermates of J20 and WT mice were euthanized at 4 or 6 months old after 3 or 5 months of Cu-containing water exposure, respectively, starting at 1 month of age. Mice were perfused with ice-cold PBS, and brains were extracted and fixed with 4% paraformaldehyde (PFA)

and cryoprotected in 30% sucrose. Thereafter, hemibrains were sectioned coronally at 40 μm using a freezing microtome (SM2010R; Leica Biosystems), and sections were stored in PBS with 0.05% sodium azide at 4°C. Sections from different mice at bregma position −2.54 mm (according to the mouse brain atlas of Franklin and Paxinos, Third Edition, 2007) were then mounted on microscopic slides and processed under the same conditions. Negative control slides were prepared by omitting primary antibodies to check for non-specific staining.

To label microglia, Iba-1 (FUJIFILM Wako Chemicals USA, Inc., catalog # 019-19741, rabbit polyclonal, 1:500 dilution) primary antibody was used. To stain for Aβ plaques, sections were pretreated with 90% formic acid for 5 mins as previously described [40, 41], before incubated in 4G8 (Covance Inc., catalog # SIG-39220, mouse monoclonal, 1:1000 dilution) Aβ plaque antibody. Microglial phenotypes at about 20 μm from the edge of the plaque (diameter ≥ 30 μm), including the area of the plaque itself and any whole microglia within the region were also assessed [41, 42]. Stained sections were imaged using confocal laser microscope (DM2500; Leica Microsystems), and microglial number and morphology were assessed using Imaris software [41, 43]

2.9. Spatial memory assessment

J20 mice and WT littermates exposed to Cu for 3 and 5 months were subjected to cognitive evaluation by object location memory (OLM) and Morris water maze (MWM) test. OLM was performed as previously described [44]. Briefly, mice were handled for 4 days and habituated to the arena, consisting of a white acrylic 5-sided box (30.5 cm x 30.5 cm x 30.5 cm) with the illumination set at ~48 LUX, for 6 consecutive days in the absence of objects. A black vertical stripe was fixed on one of the walls of the arena and the floor covered with Sani-Chips bedding. On the training day (day 7), mice were exposed to 2 identical objects (100 mL beakers filled with cement) placed at opposite ends of the arena for 10 min. Twenty-four hours later, one of the objects was moved to a novel location within the arena and mice were allowed to explore for 5 min. Objects and their relative positions were counterbalanced, and to avoid olfactory cues, objects were thoroughly cleaned with 70% ethanol and bedding was stirred after each trial. Training and trials were video recorded and hand scored by individuals blind to animal treatments. Exploration was considered as pointing the head toward an object. Turning around, chewing or sitting on the objects was not considered as exploratory behavior. The discrimination index (DI) was calculated using the formula: DI = (time spent exploring object in new location – time spent exploring object in familiar location)/(total time exploring in both locations) x 100%.

Five to seven days after OLM, mice were trained on the MWM. The maze was a circular white tank (1.28 m diameter) filled with ~22°C water and the illumination was set at ~48 LUX. The maze was located in a room containing several simple visual extra maze cues. For four days, mice were trained to find a 10.2 cm diameter circular clear Plexiglas platform submerged 1 cm beneath the surface of the water. Each day, mice received 4 training trials with inter-trial intervals of 90 sec under a warming lamp. On each trial, mice were placed into the tank at 1 of 4 designated start points in a pseudorandom order. Animals were allowed to search for the platform for a maximum of 60 sec. After reaching the platform, mice were allowed to remain there for 30 sec. If a mouse failed to find the platform within

60 sec., they were manually guided to the platform. The long-term memory test trial was performed 24 h after the last training trial and consisted of a 60 sec trial without the platform. All trials were recorded and analyzed offline using the Animal Tracker application ran in ImageJ.

3.0. Statistical analysis

All data are presented as mean ± SEM, and statistical analyses were done using GraphPad Prism 6. Values that were not within the predetermined criterion of two SDs from the mean were considered statistical outliers and were excluded from the analysis. Unpaired *t* test with Welch's correction (two-tailed) was used for comparison of means of two groups. For comparisons between three or more groups, one-way ANOVA or two-way ANOVA (for two factors) with Fisher's LSD *post hoc* test was used to evaluate statistical significance, unless otherwise stated. Data with $p < 0.05$ was considered statistically significant. To determine the number of mice needed to reach statistical difference, power analysis was conducted, and sufficient number of mice was used in this study.

3. Results

3.1. Copper exposure induces early inflammatory dyshomeostasis in microglia at pre-pathological stage

J20 mice are widely used as a transgenic mouse model of AD that develops Aβ pathology and cognitive decline at 6-8 months of age. [45]. The temporal pathological development of this mouse model was ideal for assessing Cu-induced changes in microglia activation at pre-pathological stage (4 months of age) and when Aβ pathology is developed (6 months of age). We have recently confirmed that our chronic exposure condition leads to pathological and behavioral exacerbations in J20 mice [27], thus supporting that it is an appropriate mouse model for studying the neurotoxic impact of Cu exposure through drinking water.

Corresponding to the plaque pathology, $CD68^+$ activated microglia are significantly increased in the hippocampus [46]. Notable neuronal and synapse loss are evident as early as 3 months of age and are believed to be mediated by C1q-CR3 complement cascade and excessive pruning by microglia [46, 47], suggesting pathologic activation of microglia precedes plaque pathology. We and others have previously reported that Cu exposure alters microglial phenotypes [23, 24, 26]. To further investigate the effect of Cu exposure on microglia phenotypes *in vivo*, we employed a microglia-specific TRAP on JTCx and WTCx mice (Fig. 1A) [36, 37]. These mice were exposed to either Milli-Q water (H_2O) or 1.3 ppm Cu-containing Milli-Q water (Cu) for 3 and 5 months, starting at 1 month of age. At 2 to 4 weeks before the mice were sacrificed, the mice were injected intraperitoneally to activate tamoxifen-inducible Cre/loxP recombination. In consistent with previous reports, we found clear expression of EGFP-L10a protein in microglia as early as 10 days post tamoxifen injection (data not shown) [35, 37]. The single course of tamoxifen injection led to persistent expression of EGFP-L10a for at least 27 days (Fig. 1B) in part due to the extremely low turnover rate of microglia in the brain [48, 49]. This allowed us to restrict the expression of EGFP-L10a exclusively in microglia, but not in other myeloid cell lineages with high turnover rate [35]. In addition, we did not detect EGFP-L10a expression in vehicle-injected

WTCx (Fig. 1B), which is expected in this strain of Cx3cr1^{CreER} mice used in this study [37], thereby eliminating the concern that there might be leakage of CreERT2 in the absence of tamoxifen induction.

TRAP-isolated mRNAs and their respective flow-through (unbound, UB) samples were collected for RNA-seq and translatomic analysis, after validating their RNA integrity and microglia-specificity via qPCR analysis (data not shown). TRAP-isolated mRNA was distinct from the UB samples based on PCA analysis (Fig. 1C, insert) and was enriched with microglia-specific markers, including *P2ry12, Tmem119, Hexb, Gpr34, Fcer1g, Cx3cr1, Aif1, Bin2, Cd68, Cd33, Cd74, Csf1r,* and *Trem2* (Fig. 1C), confirming enrichment of translating mRNAs from microglia origin. Together with the induction of EGFP-L10a expression only after tamoxifen administration (Fig. 1B) and that all mice injected with tamoxifen produced microglia-enriched transcripts, we demonstrated the feasibility of our TRAP technique and the reliability of our approach.

We first compared DEGs between J20 and WT mice under the control (water) treatment at both 4 and 6 months of age, in order to determine any genotype-dependent changes in the translatomic profiles within microglia. Notably, even at 4 months of age with no apparent plaque pathology in the brain, we found upregulation of genes associated with phagocytosis and cell proliferation in J20 mice (Fig. 2A, top), supporting aberrant microglia activation at pre-pathological stage of these mice [47]. At 6 months of age when plaque pathology started to build up, microglia displayed a significant upregulation of genes associated with inflammation highlighted as cellular response to TGFβ signaling, cellular response to cytokine stimulus, regulation of IκB/NF-κB signaling, lysosome signaling, endocytosis, and TNF signaling (Fig. 2A, bottom). These data further validated enrichment of transcripts from microglia and detection of microglial homeostatic changes by TRAP in a very sensitive manner.

In J20 mice, exposure to Cu further potentiated inflammatory activation of microglia in the brain. At 3 months exposure, upregulation of genes relevant to immune responses and cellular signaling, such as response to cytokine stimulus, phosphorylation, and toll-like receptor signaling pathway, were highlighted in Cu-exposed group (Fig. 2B, top). At 5 months exposure, however, these upregulated immune-related pathways were not apparent while modulation of cellular signaling cascades, such as MAPK, GTPase, and cell cycle, were upregulated in microglia from Cu-exposed J20 mice (Fig. 2B, bottom). The disappearance of immune-related pathways was probably due to the development of plaque pathology at this age and subsequent activation of inflammation in J20 mice, which mitigated the differential translatomic signatures (especially inflammation-related, as seen at 3 months exposure) triggered by Cu exposure. Yet, several chemokine genes, such as *Ccl3* and *Ccr5*, remained to be differentially upregulated by Cu exposure. Intriguingly, while WT mice exposed to Cu for 3 months downregulated several immune-related responses, such as interleukin-1 secretion, and IκB/NF-κB signaling (data not shown), WT mice with 5 months exposure clearly displayed modulation of genes responsible for immune responses highlighted as upregulation of neutrophil degranulation, endocytosis, cellular response to cytokine stimulus and downregulation of homeostatic genes (Fig. 2C, bottom). Several genes associated with degenerative phenotypes of microglia, such as *Apoe* and *Fcer1g* [31],

appeared as upregulated genes. Such appearance of upregulated immune/inflammatory genes in Cu-exposed WT mice that possess no plaque pathology signified the immunomodulatory role of Cu in the brain. These results clearly demonstrate early phenotypic and translatomic changes in microglia following chronic Cu exposure.

3.2. Copper exposure drives microglia towards degenerative phenotypes

Recent advancement on transcriptomic analysis of microglia in neurodegeneration unveiled the spectrum of activation status of microglia during the disease course. Microglia activation is classified in the range of homeostatic or neuroprotective phenotypes to degenerative phenotypes, based on the expression profile of representative genes within microglia [31, 32, 50, 51]. This targeted approach allowed us to clearly see the shift of microglia towards degenerative phenotypes. At 3 months exposure, not only the disappearance of homeostatic gene expression was noted in both WT and J20 mice exposed to Cu, an upregulation of degenerative genes was also evident in the J20 control group when compared to WT control group (Fig. 3A). This result suggests that a mixture of homeostatic and degenerative microglia co-existed at pre-pathological stage of J20 mice and was exacerbated by Cu exposure. At 5 months exposure, on the other hand, the shift was not evident in the WT mice, but more pronounced in J20 mice with more degenerative genes upregulated by Cu (Fig. 3B). Collectively, microglia-specific translatomic analysis by TRAP was capable of detecting the shift of microglial phenotypic changes in a very sensitive manner.

3.3. Chronic copper exposure exacerbates neuroinflammation and abnormalities

To predict the chronic effect of Cu exposure on microglial functions, we ran IPA using microglia-specific DEGs that were significantly altered. We first examined the biological functions and diseases profiles suggested by IPA in J20 mice to assess the effect of AD pathology on microglial translatomic profiles. As expected, the incidence of cellular and immune responses, together with diseases causing inflammation, neurology and abnormalities, were enriched as AD pathology progressed from 4 to 6 months old in J20 mice (Table 1). Intriguingly, Cu exposure exacerbated the incidence of these functions and diseases in a plaque-free condition and in a time-dependent manner as observed in Cu-exposed WT mice. On the other hand, Cu exposure to J20 mice did not seem to enhance the incidence of these profiles as much as that observed in the WT mice, although there was a time-dependent effect.

3.4. Differential microglia morphology by gender following Cu exposure

With evidence from the GO and heatmap analyses that Cu exposure activated immune responses and cellular signaling in J20 mice and directed microglia towards more degenerative phenotype at translatomic levels, we sought to assess mouse brain sections for any morphological changes in microglia. Using Iba1-immunostaining, we evaluated the surface area and numbers of positively stained microglial cells in the dentate gyrus (DG) and cortical (Ctx) regions of 3 and 5 months Cu exposed J20 mice (Fig. 4A and B). While the surface area of $Iba1^+$ microglial cells was not altered (data not shown), the number of cells were significantly elevated in the male mice, but not females (Fig. 4A and B). We have also assessed $Iba1^+$ microglial phenotypes around $4G8^+$ plaques on 5 months exposure J20 mice, but did not find significant alteration in the count and morphology (Fig. 4C - F) at this early

plaque stage. Interestingly, Cu exposed J20 female mice exhibited the least count, total processes length and branching of Iba1$^+$ microglia among the exposed groups.

3.5. Copper exposure exacerbates cognitive decline

We found a significant impairment of cognition, assessed by OLM, in WT mice exposed to Cu for 5 months (Fig. 5A). This result is consistent with our previous findings in 9 months Cu exposure in WT mice [27], highlighting the progressive cognitive decline associated with the duration of Cu exposure. J20 mice, on the other hand, did not exhibit worsened cognition by Cu, but already showing a substantial impairment due to overexpression of familial AD mutations (Fig. 5A). Similarly in Morris water maze test, J20 mice consistently displayed impaired cognitive function, while adverse effect by Cu exposure disappeared in WT mice (Fig. 5B, C). This is in part due to the sensitivity and other confounding factors found in the Morris water maze test [44].

4. Discussion

Our results support that microglia-enriched translatomic analysis by TRAP is a highly sensitive method that identifies early changes in microglia homeostasis and degenerative activation, even before the appearance of clear morphological changes of activated microglia, such as shorter processes and less branching, and plaque pathology in the brain. TRAP is particularly useful for this study because microglia constitute less than 10% of the brain cell populations that subtle alterations in the transcription may be masked by the whole brain transcripts [39]. We have, in fact, observed the disappearance of the distinctive homeostasis and degenerative gene signatures when using the whole brain transcripts for analysis (data not shown). Another advantage of this technique is that translating mRNA are being isolated, thereby providing the translatomic profile that correlates better with proteomics than that of the transcriptomes [52].

Chronic exposure to environmental contaminants is one of the suspected environmental risk factors for developing AD. One particular contaminants of concern is the exposure to the poorly metabolized inorganic cupric Cu^{2+} ions that is found leaking from the Cu water pipes into our tap water [13, 53]. Several animal studies have shown that chronic Cu exposure through drinking water, even at trace level, aggravates Aβ plaque pathology [17, 18]. While several putative mechanisms by which Cu exacerbates AD pathology have been reported, its influence on microglia phenotypes, especially upon chronic exposure at the levels allowed in drinking water by the U.S. regulatory agent, has not been evaluated in details. Our results indicate that Cu exposure substantially drives microglia towards degenerative phenotypes at translational levels, even in WT mice and pre-pathological stage of J20 mice. Such phenotypes could contribute to accelerated degenerative processes including excessive synapse pruning and neuronal loss [33, 47], secretion of pro-inflammatory cytokines and oxidative damage [54-56], impairment of effective containment of Aβ [32, 57], and subsequent cognitive decline.

It is worth noting that Cu deficiency also resulted in aberrant microglial activation that contributed to neurodegenerative diseases, implicating that Cu plays a critical role in maintaining microglia homeostasis [30]. Notwithstanding that, studies have shown that

differential activation of microglial phenotypes and toxicity in the brain depend on the valency of Cu (review in [58]). For instance, the cuprous Cu^{+} ion polarizes murine BV2 cells from a pro-inflammatory phenotype to an anti-inflammatory state by inhibiting nitric oxide production [59]. In contrast, we show that the cupric Cu^{2+} form impairs phagocytosis and elevates the release of pro-inflammatory cytokines, such as IL-1β, IL-6 and TNFα, of Aβ-stimulated BV2 cells [24], thus substantiating that the Cu^{2+} form perturbs inflammatory responses as observed in this study.

The expression profile determined by the translatomic analysis was not necessarily reflected by the morphological changes in microglia of Cu-exposed J20 mice. The overall shapes of microglia and their processes appeared unaffected in the brain regions we examined. However, we found significantly higher number of $Ibal^{+}$ microglia in J20 female mice than the males, as reported in WT C57BL/6J mice [60]. Perhaps owing to the lower basal number of $Ibal^{+}$ microglia in control males, Cu exposure has the propensity to recruit more $Ibal^{+}$ microglia to the corresponding brain regions in the male mice, as it seemed to be already high baseline in the females. On the other hand, when assessing the morphology of $Iba1^{+}$ microglia around $4G8^{+}$ Aβ plaques in 6-month old J20 mice, the female mice exhibited more degenerative phenotypes of microglia morphology by displaying more amoeboid features, such as presenting the shortest processes length and least microglia branching among all groups. It is noteworthy to point out that microglia from female $APP^{NL\text{-}G\text{-}F}$-KI mice tend to progress to the AD-associated activated state earlier than the male counterparts with the dimorphism being more pronounced in older mice [61]. It is thus intriguing to report that chronic Cu exposure alone shows tendency to trigger early degenerative phenotypes of microglia in female mice, while the morphology of plaque-associated microglia between genders of young J20 mice is not yet different in our study. Interestingly, the gender effect did not seem to have masked the adverse effect of Cu exposure in J20 mice when assessed at the translatomic level and in the behavioral tasks.

While there might be a possibility that the shift in microglial translatomic profiles would not be reflected in their morphological changes in WT mice, the same analysis as J20 mice will still be interesting to sought after in follow-up experiments. This will allow the assessment of the influence of chronic Cu exposure on microglia morphology in the absence of plaque pathology, and if there will be any gender differences in the modulation. In another note, we postulate that there might be differences in the brain Cu levels between genotypes or genders following the chronic Cu exposure. This is another conceivable explanation to further address the observed phenotypes. We plan to quantitatively analyze the levels of Cu and other trace metals in the mouse brains using ICP-MS in follow-up studies.

In summary, our findings unveil that chronic Cu exposure at environmentally relevant dose perturbs microglial homeostasis in both plaque-free and early plaque stages of J20 mice as well as in WT mice. Excess Cu intake through drinking water shifts microglial expression profile towards degenerative phenotypes, which may in part contribute to accelerated cognitive impairment observed in these mice. The employment of the highly sensitive microglia-specific translatomic analysis allows early tracking of translational alterations induced by Cu exposure and AD pathology, before the appearance of Aβ plaques or microglial morphological changes.

Acknowledgements

We thank the following people for their kind contribution and assistance: Diana Nguyen Tran and Christine Chen (University of California, Merced) for their assistance in the animal exposure; Dr. Sakura Minami and Dr. Li Gan (Gladstone Institute of Neurological Disease at University of California, San Francisco) for their protocol on the preparation of tamoxifen and injection regimen for inducing Cre-mediated recombination; Dr. Christopher Parkhurst and Dr. Wen-Biao Gan (New York University School of Medicine) for their protocol on microglia isolation using Percoll gradient; The Genomic High-Throughput Facility (University of California, Irvine) for running bulk RNA-sequencing with support, in part, from the Genomics High Throughput Facility Shared Resource of the Cancer Center Support Grant (P30CA-062203) and the NIH shared instrumentation grants (1S10RR025496-01, 1S10OD010794-01, and 1S10OD021718-01).

Funding

This work was supported by the National Institutes of Health [R01 ES024331, MK and RF1 AG054011, PA], the Alzheimer's Association [AARF-16-440554, SLL], and the National Alliance for Research on Schizophrenia and Depression [25065, PA].

Abbreviations

Cu	Copper
AD	Alzheimer’s disease
WT	Wild-type
TRAP	Translating ribosome affinity purification
Aβ	Amyloid-β
CSF	Cerebrospinal fluid
MCI	Mild cognitive impairment
CNS	Central nervous system
Cu^{+}	Cuprous copper
Cu^{2+}	Inorganic cupric copper
APP	Amyloid precursor protein
LRP1	Low-density lipoprotein-like receptor protein 1
Cre-ERT2	Tamoxifen-inducible Cre recombinase
EYFP	Enhanced yellow fluorescent protein
IRES	Internal ribosome entry site
JTCx	J20/TRAP/Cx3cr1
WTCx	WT/TRAP/Cx3cr1
H_2O	Milli-Q water
$CUCl_2.2H_2O$	Copper (II) chloride dehydrate

PBS	Phosphate buffered saline
PFH	PBS/fetal calf serum/HEPES
DPBS	Dulbecco's Phosphate-Buffered Saline
HEPES	4-(2-hydroxyethyl)-l-piperazineethanesulfonic acid
EDTA	Ethylenediaminetetraacetic acid
SDS-PAGE	Sodium dodecyl sulphate-polyacrylamide gel electrophoresis
PVDF	Polyvinylidene fluoride
GFP	Green fluorescent protein
GAPDH	Glyceraldehyde 3-phosphate dehydrogenase
TBST	Tris-buffered saline with 0.1% Tween 20
KCl	Potassium chloride
$MgCl_2$	Magnesium chloride
DTT	Dithiothreitol
NP-40	Nonylphenyl-polyethylene glycol
DHPC	1,2-diheptanoyl-sn-glycero-3-phosphocholine
UB	Unbound
qPCR	Quantitative polymerase chain reaction
RIN	RNA integrity number
RNA-seq	RNA sequencing
FPKM	Fragments Per Kilobase of transcript per Million mapped reads
PCA	Principal component analysis
DEGs	Differentially expressed genes
GO	Gene Ontology
IPA	Ingenuity Pathway Analysis
PFA	Paraformaldehyde
OLM	Object location memory
MWM	Morris water maze
DI	Discrimination index

DG	Dentate gyrus
Ctx	Cortex
M	Male
F	Female

References

[1]. Gatz M, Pedersen NL, Berg S, Johansson B, Johansson K, Mortimer JA, Posner SF, Viitanen M, Winblad B, Ahlbom A, Heritability for Alzheimer's disease: the study of dementia in Swedish twins, J Gerontol A Biol Sci Med Sci 52(2) (1997) M117–25. [PubMed: 9060980]

[2]. Gatz M, Reynolds CA, Fratiglioni L, Johansson B, Mortimer JA, Berg S, Fiske A, Pedersen NL, Role of genes and environments for explaining Alzheimer disease, Archives of general psychiatry 63(2) (2006) 168–74. [PubMed: 16461860]

[3]. Squitti R, Barbati G, Rossi L, Ventriglia M, Dal Forno G, Cesaretti S, Moffa F, Caridi I, Cassetta E, Pasqualetti P, Calabrese L, Lupoi D, Rossini PM, Excess of nonceruloplasmin serum copper in AD correlates with MMSE, CSF [beta]-amyloid, and h-tau, Neurology 67(1) (2006) 76–82. [PubMed: 16832081]

[4]. Vural H, Demirin H, Kara Y, Eren I, Delibas N, Alterations of plasma magnesium, copper, zinc, iron and selenium concentrations and some related erythrocyte antioxidant enzyme activities in patients with Alzheimer's disease, J Trace Elem Med Biol 24(3) (2010) 169–73. [PubMed: 20569929]

[5]. Ventriglia M, Bucossi S, Panetta V, Squitti R, Copper in Alzheimer's disease: a meta-analysis of serum, plasma, and cerebrospinal fluid studies, J Alzheimers Dis 30(4) (2012) 981–4. [PubMed: 22475798]

[6]. Wang ZX, Tan L, Wang HF, Ma J, Liu J, Tan MS, Sun JH, Zhu XC, Jiang T, Yu JT, Serum Iron, Zinc, and Copper Levels in Patients with Alzheimer's Disease: A Replication Study and Meta-Analyses, J Alzheimers Dis 47(3) (2015) 565–81. [PubMed: 26401693]

[7]. Talwar P, Grover S, Sinha J, Chandna P, Agarwal R, Kushwaha S, Kukreti R, Multifactorial Analysis of a Biomarker Pool for Alzheimer Disease Risk in a North Indian Population, Dement Geriatr Cogn Disord 44(1-2) (2017) 25–34. [PubMed: 28633142]

[8]. Squitti R, Ghidoni R, Siotto M, Ventriglia M, Benussi L, Paterlini A, Magri M, Binetti G, Cassetta E, Caprara D, Vernieri F, Rossini PM, Pasqualetti P, Value of serum nonceruloplasmin copper for prediction of mild cognitive impairment conversion to Alzheimer disease, Ann Neurol 75(4) (2014) 574–80. [PubMed: 24623259]

[9]. Squitti R, Ghidoni R, Scrascia F, Benussi L, Panetta V, Pasqualetti P, Moffa F, Bernardini S, Ventriglia M, Binetti G, Rossini PM, Free copper distinguishes mild cognitive impairment subjects from healthy elderly individuals, J Alzheimers Dis 23(2) (2011) 239–48. [PubMed: 20930297]

[10]. Salustri C, Barbati G, Ghidoni R, Quintiliani L, Ciappina S, Binetti G, Squitti R, Is cognitive function linked to serum free copper levels? A cohort study in a normal population, Clin Neurophysiol 121(4) (2010) 502–7. [PubMed: 20097602]

[11]. Silbert LC, Lahna D, Promjunyakul NO, Boespflug E, Ohya Y, Higashiuesato Y, Nishihira J, Katsumata Y, Tokashiki T, Dodge HH, Risk Factors Associated with Cortical Thickness and White Matter Hyperintensities in Dementia Free Okinawan Elderly, J Alzheimers Dis 63(1) (2018) 365–372. [PubMed: 29578488]

[12]. Morris MC, Evans DA, Tangney CC, Bienias JL, Schneider JA, Wilson RS, Scherr PA, Dietary copper and high saturated and trans fat intakes associated with cognitive decline, Archives of neurology 63(8) (2006) 1085–8. [PubMed: 16908733]

[13]. Brewer GJ, Copper-2 Ingestion, Plus Increased Meat Eating Leading to Increased Copper Absorption, Are Major Factors Behind the Current Epidemic of Alzheimer's Disease, Nutrients 7(12)(2015) 10053–64. [PubMed: 26633489]

[14]. Ceko MJ, Aitken JB, Harris HH, Speciation of copper in a range of food types by X-ray absorption spectroscopy, Food Chem 164 (2014) 50–4. [PubMed: 24996304]

[15]. Prohaska JR, Role of copper transporters in copper homeostasis, Am J Clin Nutr 88(3) (2008) 826S–9S. [PubMed: 18779302]

[16]. Hill GM, Brewer GJ, Juni JE, Prasad AS, Dick RD, Treatment of Wilson's disease with zinc. II. Validation of oral 64copper with copper balance, Am J Med Sci 292(6) (1986) 344–9. [PubMed: 3799705]

[17]. Sparks DL, Friedland R, Petanceska S, Schreurs BG, Shi J, Perry G, Smith MA, Sharma A, Derosa S, Ziolkowski C, Stankovic G, Trace copper levels in the drinking water, but not zinc or aluminum influence CNS Alzheimer-like pathology, The journal of nutrition, health & aging 10(4) (2006) 247–54.

[18]. Sparks DL, Schreurs BG, Trace amounts of copper in water induce beta-amyloid plaques and learning deficits in a rabbit model of Alzheimer's disease, Proceedings of the National Academy of Sciences of the United States of America 100(19) (2003) 11065–9. [PubMed: 12920183]

[19]. Cherny RA, Atwood CS, Xilinas ME, Gray DN, Jones WD, McLean CA, Barnham KJ, Volitakis I, Fraser FW, Kim Y, Huang X, Goldstein LE, Moir RD, Lim JT, Beyreuther K, Zheng H, Tanzi RE, Masters CL, Bush AI, Treatment with a copper-zinc chelator markedly and rapidly inhibits beta-amyloid accumulation in Alzheimer's disease transgenic mice, Neuron 30(3) (2001) 665–76. [PubMed: 11430801]

[20]. Gerber H, Wu F, Dimitrov M, Garcia Osuna GM, Fraering PC, Zinc and Copper Differentially Modulate Amyloid Precursor Protein Processing by gamma-Secretase and Amyloid-beta Peptide Production, The Journal of biological chemistry 292(9) (2017) 3751–3767. [PubMed: 28096459]

[21]. Matlack KE, Tardiff DF, Narayan P, Hamamichi S, Caldwell KA, Caldwell GA, Lindquist S, Clioquinol promotes the degradation of metal-dependent amyloid-beta (Abeta) oligomers to restore endocytosis and ameliorate Abeta toxicity, Proceedings of the National Academy of Sciences of the United States of America 111(11) (2014) 4013–8. [PubMed: 24591589]

[22]. Crouch PJ, Hung LW, Adlard PA, Cortes M, Lal V, Filiz G, Perez KA, Nurjono M, Caragounis A, Du T, Laughton K, Volitakis I, Bush AI, Li QX, Masters CL, Cappai R, Cherny RA, Donnelly PS, White AR, Barnham KJ, Increasing Cu bioavailability inhibits Abeta oligomers and tau phosphorylation, Proceedings of the National Academy of Sciences of the United States of America 106(2) (2009) 381–6. [PubMed: 19122148]

[23]. Kitazawa M, Cheng D, Laferla FM, Chronic copper exposure exacerbates both amyloid and tau pathology and selectively dysregulates cdk5 in a mouse model of AD, Journal of neurochemistry 108(6) (2009) 1550–60. [PubMed: 19183260]

[24]. Kitazawa M, Hsu HW, Medeiros R, Copper exposure perturbs brain inflammatory responses and impairs clearance of amyloid-beta, Toxicol Sci 152(1) (2016) 194–204. [PubMed: 27122238]

[25]. Yu J, Luo X, Xu H, Ma Q, Yuan J, Li X, Chang RC, Qu Z, Huang X, Zhuang Z, Liu J, Yang X, Identification of the key molecules involved in chronic copper exposure-aggravated memory impairment in transgenic mice of Alzheimer's disease using proteomic analysis, J Alzheimers Dis 44(2) (2015) 455–69. [PubMed: 25352456]

[26]. Zheng Z, White C, Lee J, Peterson TS, Bush AI, Sun GY, Weisman GA, Petris MJ, Altered microglial copper homeostasis in a mouse model of Alzheimer's disease, Journal of neurochemistry 114(6) (2010) 1630–8. [PubMed: 20626553]

[27]. Hsu HW, Rodriguez-Ortiz CJ, Lim SL, Zumkehr J, Kilian JG, Vidal J, Kitazawa M, Copper-Induced Upregulation of MicroRNAs Directs the Suppression of Endothelial LRP1 in Alzheimer's Disease Model, Toxicol Sci 170(1) (2019) 144–156. [PubMed: 30923833]

[28]. Singh I, Sagare AP, Coma M, Perlmutter D, Gelein R, Bell RD, Deane RJ, Zhong E, Parisi M, Ciszewski J, Kasper RT, Deane R, Low levels of copper disrupt brain amyloid-beta homeostasis by altering its production and clearance, Proceedings of the National Academy of Sciences of the United States of America 110(36) (2013) 14771–6. [PubMed: 23959870]

[29]. Bayer TA, Schafer S, Simons A, Kemmling A, Kamer T, Tepest R, Eckert A, Schussel K, Eikenberg O, Sturchler-Pierrat C, Abramowski D, Staufenbiel M, Multhaup G, Dietary Cu stabilizes brain superoxide dismutase 1 activity and reduces amyloid Abeta production in APP23 transgenic mice, Proceedings of the National Academy of Sciences of the United States of America 100(24) (2003) 14187–92. [PubMed: 14617773]

[30]. Zucconi GG, Cipriani S, Scattoni R, Balgkouranidou I, Hawkins DP, Ragnarsdottir KV, Copper deficiency elicits glial and neuronal response typical of neurodegenerative disorders, Neuropathol Appl Neurobiol 33(2) (2007) 212–25. [PubMed: 17359362]

[31]. Butovsky O, Jedrychowski MP, Moore CS, Cialic R, Lanser AJ, Gabriely G, Koeglsperger T, Dake B, Wu PM, Doykan CE, Fanek Z, Liu L, Chen Z, Rothstein JD, Ransohoff RM, Gygi SP, Antel JP, Weiner HL, Identification of a unique TGF-beta-dependent molecular and functional signature in microglia, Nature neuroscience 17(1) (2014) 131–43. [PubMed: 24316888]

[32]. Spangenberg E, Severson PL, Hohsfield LA, Crapser J, Zhang J, Burton EA, Zhang Y, Spevak W, Lin J, Phan NY, Habets G, Rymar A, Tsang G, Walters J, Nespi M, Singh P, Broome S, Ibrahim P, Zhang C, Bollag G, West BL, Green KN, Sustained microglial depletion with CSF1R inhibitor impairs parenchymal plaque development in an Alzheimer's disease model, Nature communications 10(1) (2019) 3758.

[33]. Spangenberg EE, Lee RJ, Najafi AR, Rice RA, Elmore MR, Blurton-Jones M, West BL, Green KN, Eliminating microglia in Alzheimer's mice prevents neuronal loss without modulating amyloid-beta pathology, Brain 139(Pt 4) (2016) 1265–81. [PubMed: 26921617]

[34]. Wang Y, Ulland TK, Ulrich JD, Song W, Tzaferis JA, Hole JT, Yuan P, Mahan TE, Shi Y, Gilfillan S, Cella M, Grutzendler J, DeMattos RB, Cirrito JR, Holtzman DM, Colonna M, TREM2-mediated early microglial response limits diffusion and toxicity of amyloid plaques, J Exp Med 213(5) (2016) 667–75. [PubMed: 27091843]

[35]. Parkhurst CN, Yang G, Ninan I, Savas JN, Yates JR 3rd, Lafaille JJ, Hempstead BL, Littman DR, Gan WB, Microglia promote learning-dependent synapse formation through brain-derived neurotrophic factor, Cell 155(7) (2013) 1596–609. [PubMed: 24360280]

[36]. Zhou P, Zhang Y, Ma Q, Gu F, Day DS, He A, Zhou B, Li J, Stevens SM, Romo D, Pu WT, Interrogating translational efficiency and lineage-specific transcriptomes using ribosome affinity purification, Proceedings of the National Academy of Sciences of the United States of America 110(38) (2013) 15395–400. [PubMed: 24003143]

[37]. Ayata P, Badimon A, Strasburger HJ, Duff MK, Montgomery SE, Loh YE, Ebert A, Pimenova AA, Ramirez BR, Chan AT, Sullivan JM, Purushothaman I, Scarpa JR, Goate AM, Busslinger M, Shen L, Losic B, Schaefer A, Epigenetic regulation of brain region-specific microglia clearance activity, Nature neuroscience 21(8) (2018) 1049–1060. [PubMed: 30038282]

[38]. Zhan L, Krabbe G, Du F, Jones I, Reichert MC, Telpoukhovskaia M, Kodama L, Wang C, Cho SH, Sayed F, Li Y, Le D, Zhou Y, Shen Y, West B, Gan L, Proximal recolonization by self-renewing microglia re-establishes microglial homeostasis in the adult mouse brain, PLoS Biol 17(2) (2019) e3000134. [PubMed: 30735499]

[39]. Heiman M, Kulicke R, Fenster RJ, Greengard P, Heintz N, Cell type-specific mRNA purification by translating ribosome affinity purification (TRAP), Nat Protoc 9(6) (2014) 1282–91. [PubMed: 24810037]

[40]. Kitazawa M, Cheng D, Tsukamoto MR, Koike MA, Wes PD, Vasilevko V, Cribbs DH, LaFerla FM, Blocking IL-1 signaling rescues cognition, attenuates tau pathology, and restores neuronal beta-catenin pathway function in an Alzheimer's disease model, J Immunol 187(12) (2011) 6539–49. [PubMed: 22095718]

[41]. Lim SL, Tran DN, Zumkehr J, Chen C, Ghiaar S, Kieu Z, Villanueva E, Gallup V, Rodriguez-Ortiz CJ, Kitazawa M, Inhibition of hematopoietic cell kinase dysregulates microglial function and accelerates early stage Alzheimer's disease-like neuropathology, Glia 66(12) (2018) 2700–18. [PubMed: 30277607]

[42]. Ulrich JD, Finn MB, Wang Y, Shen A, Mahan TE, Jiang H, Stewart FR, Piccio L, Colonna M, Holtzman DM, Altered microglial response to Abeta plaques in APPPS1-21 mice heterozygous for TREM2, Molecular neurodegeneration 9 (2014) 20. [PubMed: 24893973]

[43]. Marsh SE, Abud EM, Lakatos A, Karimzadeh A, Yeung ST, Davtyan H, Fote GM, Lau L, Weinger JG, Lane TE, Inlay MA, Poon WW, Blurton-Jones M, The adaptive immune system restrains Alzheimer's disease pathogenesis by modulating microglial function, Proceedings of the National Academy of Sciences of the United States of America 113(9) (2016) E1316–25. [PubMed: 26884167]

[44]. Vogel-Ciernia A, Wood MA, Examining object location and object recognition memory in mice, Curr Protoc Neurosci 69 (2014) 8 31 1–17. [PubMed: 25297693]

[45]. Mucke L, Masliah E, Yu GQ, Mallory M, Rockenstein EM, Tatsuno G, Hu K, Kholodenko D, Johnson-Wood K, McConlogue L, High-level neuronal expression of abeta 1-42 in wild-type human amyloid protein precursor transgenic mice: synaptotoxicity without plaque formation, J Neurosci 20(11) (2000) 4050–8. [PubMed: 10818140]

[46]. Wright AL, Zinn R, Hohensinn B, Konen LM, Beynon SB, Tan RP, Clark IA, Abdipranoto A, Vissel B, Neuroinflammation and neuronal loss precede Abeta plaque deposition in the hAPP-J20 mouse model of Alzheimer's disease, PloS one 8(4) (2013) e59586. [PubMed: 23560052]

[47]. Hong S, Beja-Glasser VF, Nfonoyim BM, Frouin A, Li S, Ramakrishnan S, Merry KM, Shi Q, Rosenthal A, Barres BA, Lemere CA, Selkoe DJ, Stevens B, Complement and microglia mediate early synapse loss in Alzheimer mouse models, Science (New York, N.Y 352(6286) (2016) 712–6.

[48]. Lawson LJ, Perry VH, Gordon S, Turnover of resident microglia in the normal adult mouse brain, Neuroscience 48(2) (1992) 405–15. [PubMed: 1603325]

[49]. van Furth R, Cohn ZA, The origin and kinetics of mononuclear phagocytes, J Exp Med 128(3) (1968) 415–35. [PubMed: 5666958]

[50]. Bonham LW, Sirkis DW, Yokoyama JS, The Transcriptional Landscape of Microglial Genes in Aging and Neurodegenerative Disease, Front Immunol 10 (2019) 1170. [PubMed: 31214167]

[51]. Mathys H, Davila-Velderrain J, Peng Z, Gao F, Mohammadi S, Young JZ, Menon M, He L, Abdurrob F, Jiang X, Martorell AJ, Ransohoff RM, Hafler BP, Bennett DA, Kellis M, Tsai LH, Single-cell transcriptomic analysis of Alzheimer's disease, Nature 570(7761) (2019) 332–337. [PubMed: 31042697]

[52]. Kitchen RR, Rozowsky JS, Gerstein MB, Nairn AC, Decoding neuroproteomics: integrating the genome, translatome and functional anatomy, Nature neuroscience 17(11) (2014) 1491–9. [PubMed: 25349915]

[53]. Brewer GJ, Copper-2 Hypothesis for Causation of the Current Alzheimer's Disease Epidemic Together with Dietary Changes That Enhance the Epidemic, Chem Res Toxicol 30(3) (2017) 763–768. [PubMed: 28161940]

[54]. Combs CK, Karlo JC, Kao SC, Landreth GE, beta-Amyloid stimulation of microglia and monocytes results in TNFalpha-dependent expression of inducible nitric oxide synthase and neuronal apoptosis, J Neurosci 21(4) (2001) 1179–88. [PubMed: 11160388]

[55]. McDonald DR, Brunden KR, Landreth GE, Amyloid fibrils activate tyrosine kinase-dependent signaling and superoxide production in microglia, J Neurosci 17(7) (1997) 2284–94. [PubMed: 9065490]

[56]. Smith JA, Das A, Ray SK, Banik NL, Role of pro-inflammatory cytokines released from microglia in neurodegenerative diseases, Brain Res Bull 87(1) (2012) 10–20. [PubMed: 22024597]

[57]. Yuan P, Condello C, Keene CD, Wang Y, Bird TD, Paul SM, Luo W, Colonna M, Baddeley D, Grutzendler J, TREM2 Haplodeficiency in Mice and Humans Impairs the Microglia Barrier Function Leading to Decreased Amyloid Compaction and Severe Axonal Dystrophy, Neuron 90(4) (2016) 724–39. [PubMed: 27196974]

[58]. Hsu HW, Bondy SC, Kitazawa M, Environmental and Dietary Exposure to Copper and Its Cellular Mechanisms Linking to Alzheimer's Disease, Toxicol Sci 163(2) (2018) 338–345. [PubMed: 29409005]

[59]. Rossi-George A, Guo CJ, Oakes BL, Gow AJ, Copper modulates the phenotypic response of activated BV2 microglia through the release of nitric oxide, Nitric Oxide 27(4) (2012) 201–9. [PubMed: 22819698]

[60]. Mouton PR, Long JM, Lei DL, Howard V, Jucker M, Calhoun ME, Ingram DK, Age and gender effects on microglia and astrocyte numbers in brains of mice, Brain Res 956(1) (2002) 30–5. [PubMed: 12426043]

[61]. Sala Frigerio C, Wolfs L, Fattorelli N, Thrupp N, Voytyuk I, Schmidt I, Mancuso R, Chen WT, Woodbury ME, Srivastava G, Moller T, Hudry E, Das S, Saido T, Karran E, Hyman B, Perry VH, Fiers M, De Strooper B, The Major Risk Factors for Alzheimer's Disease: Age, Sex, and Genes Modulate the Microglia Response to Abeta Plaques, Cell Rep 27(4) (2019) 1293–1306 e6. [PubMed: 31018141]

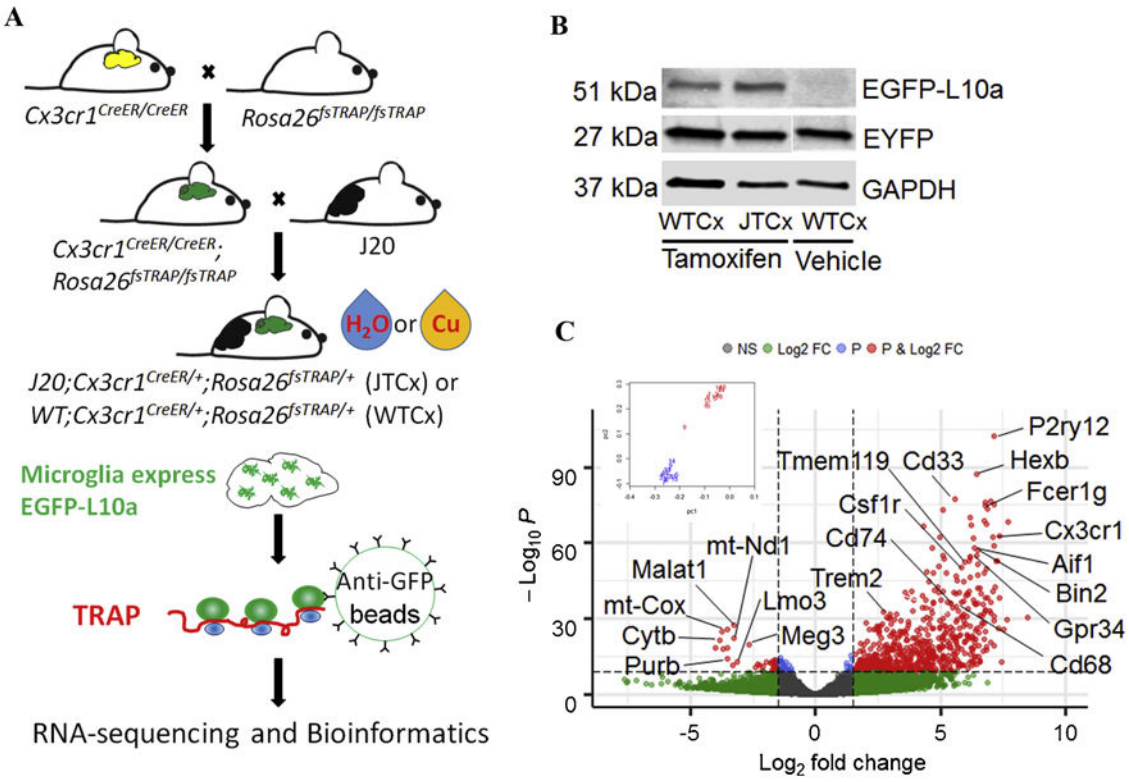

Figure 1. Microglia-enriched translatomic analysis by TRAP.

(A) Schematic diagram illustrating the experimental design for microglia-specific mRNA isolation by TRAP and RNA-sequencing. **(B)** Expression of EGFP-L10a in WTCx and JTCx mice at 27 days after tamoxifen intraperitoneal injection. Littermates were injected with either tamoxifen (2 mg/day) or vehicle (100 μl corn oil) for 5 consecutive days. Protein lysates were extracted from microglia in hemi-brains of each genotype (n = 3 per group). Representative image of the Western analysis was shown here. All microglial lysates expressed EYFP as it co-expressed with Cre-ERT2. On the other hand, only mice injected with tamoxifen expressed EFGP-L10a owing to Cre-mediated recombination, denoting that tamoxifen administration was necessary to induce EFGP-L10a expression and there is no leakage of CreERT2 without tamoxifen induction. **(C)** Principle component analysis (PCA, Inset) showed distinct clusters of TRAP (red) and unbound flow-through (UB, blue) samples. Volcano plot revealed enrichment of microglia-specific genes and depletion of genes from other cell types, validating the feasibility of our TRAP technique.

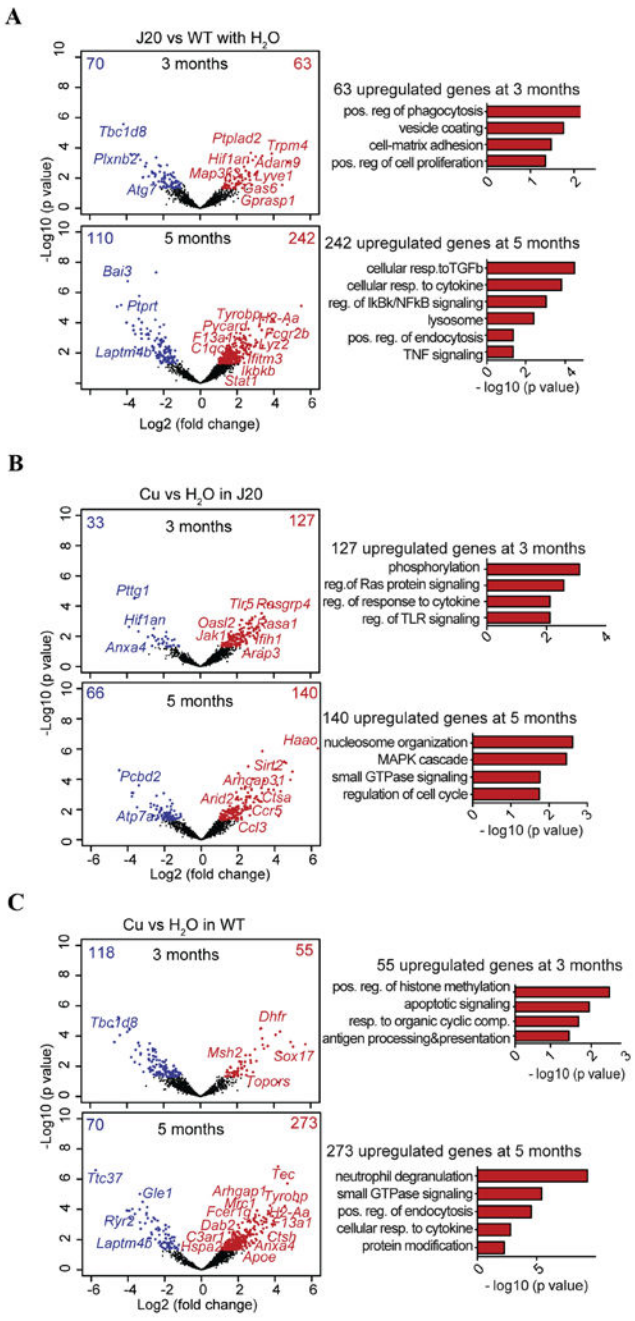

Figure 2. Microglia-enriched RNA-seq and analysis by genotype and by Cu exposure in mice.

Volcano plots of up- and down-regulated genes and Gene Ontology (GO) term enrichment analysis (right) showing microglia-specific differential gene expression levels and upregulated cellular networks of **(A)** 4-month (top) and 6-month (bottom) old J20 vs. WT mice; **(B)** Cu- vs. water-exposed J20 mice for 3 months (top) and 5 months (bottom); and **(C)** Cu- vs. water-exposed WT mice for 3 months (top) and 5 months (bottom). n = 3-4 mice per treatment group.

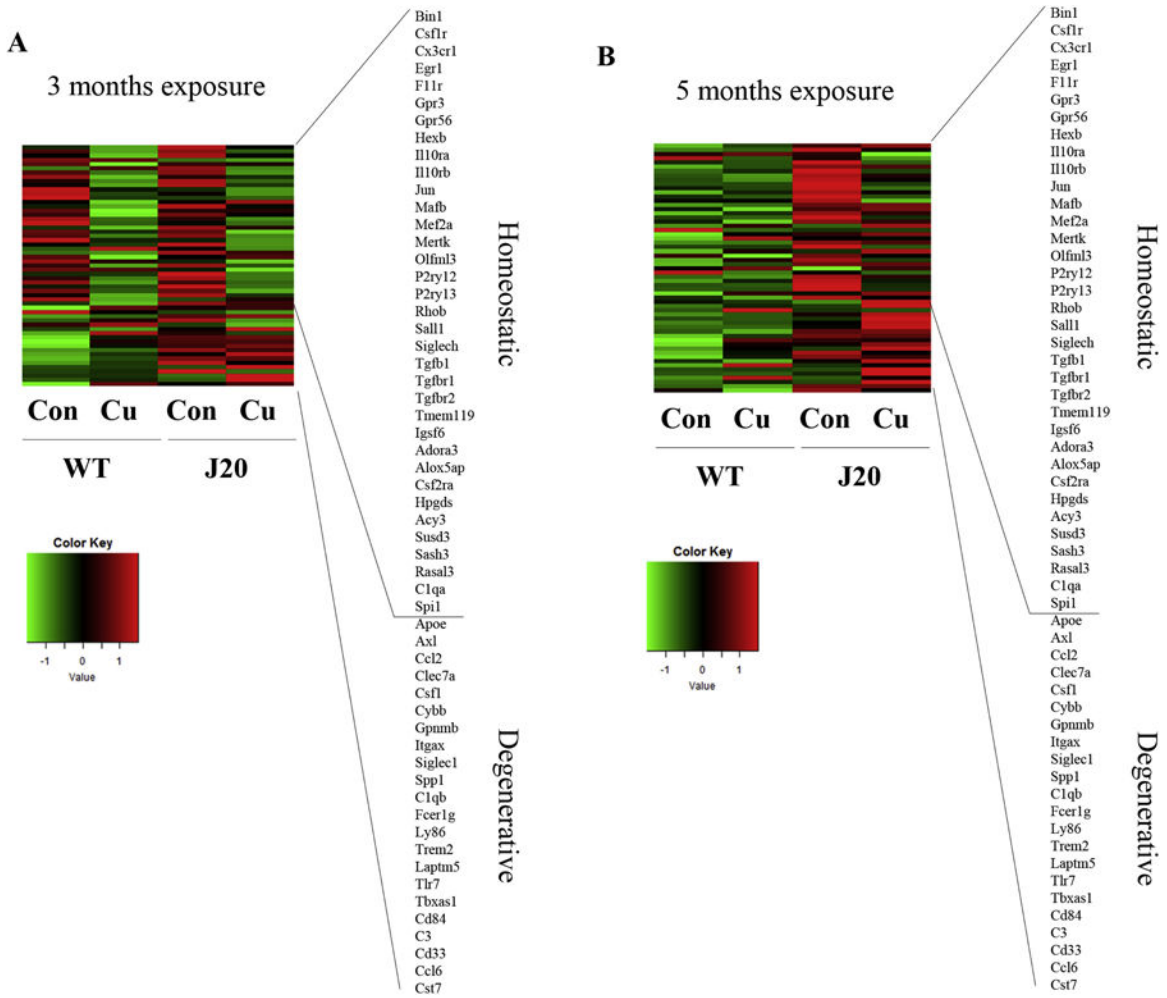

Figure 3. Cu exposure drives microglia towards degenerative expression profile.

(A) Heatmap showing homeostatic and degenerative translatomic signatures in microglia after 3 months Cu exposure to WT and J20 mice. Cu exposure attenuated expression of homeostatic genes in both WT and J20 mice, and elevated that of degenerative genes in J20 mice when compared to WT control (con; water exposed) mice. **(B)** Heatmap showing homeostatic and degenerative translatomic signatures in microglia after 5 months Cu exposure to WT and J20 mice. Cu exposure drove microglia phenotypic shift from homeostatic to degenerative in J20 mice.

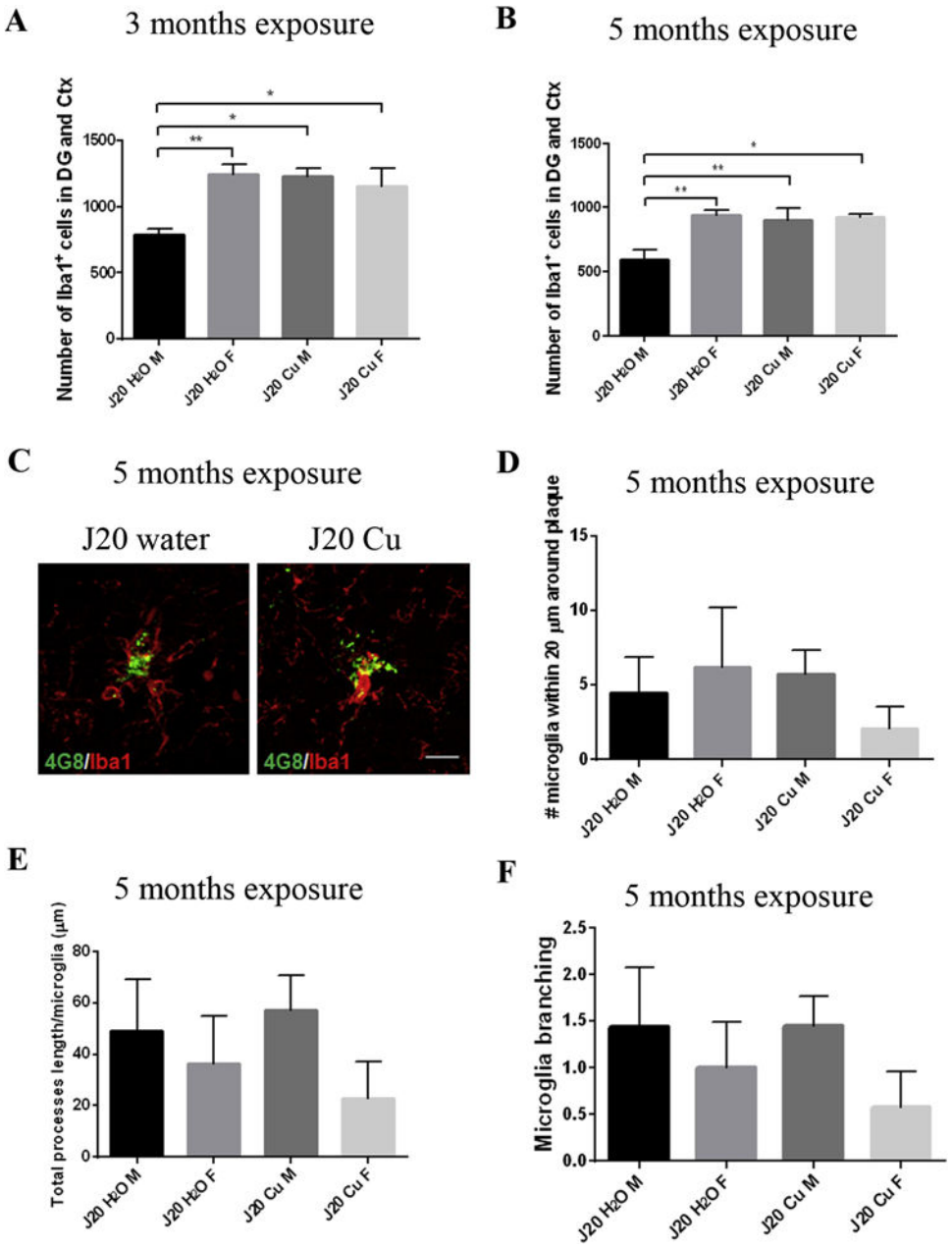

Figure 4. Microglia morphology in the brain following Cu exposure.

Number of Iba1$^+$ microglia in dentate gyrus (DG) and cortical (Ctx) regions of **(A)** 3 months and **(B)** 5 months exposed (H_2O or Cu) J20 mice. Data were stratified by genders – male (M) and female (F). Cu exposure significantly elevated number of Iba1$^+$ microglial cells in combined regions of DG and Ctx of male mice, but not in the female mice. Data are expressed as mean ± SEM from 2-8 mice per gender per treatment group with one section per mouse. *$p < 0.05$ and **$p < 0.01$ relative to J20 control male mice. **(C)** Representative images of Iba1$^+$ microglial cells (red) clustering around 4G8$^+$ plaques (green) in 5 months exposed J20 female mice. Scale bar at 20 µm. **(D)** Number of Iba1$^+$ microglial cells localizing within 20 µm from the edge of 4G8$^+$ plaques in H_2O or Cu exposed male (M) and

female (F) J20 mice were counted. **(E)** Total processes length of Iba1$^+$ microglial cells per microglia and **(F)** branching of Iba1$^+$ microglial cells around plaques were also assessed. Data are expressed as mean ± SEM from 2-6 mice per gender per treatment group with one section per mouse.

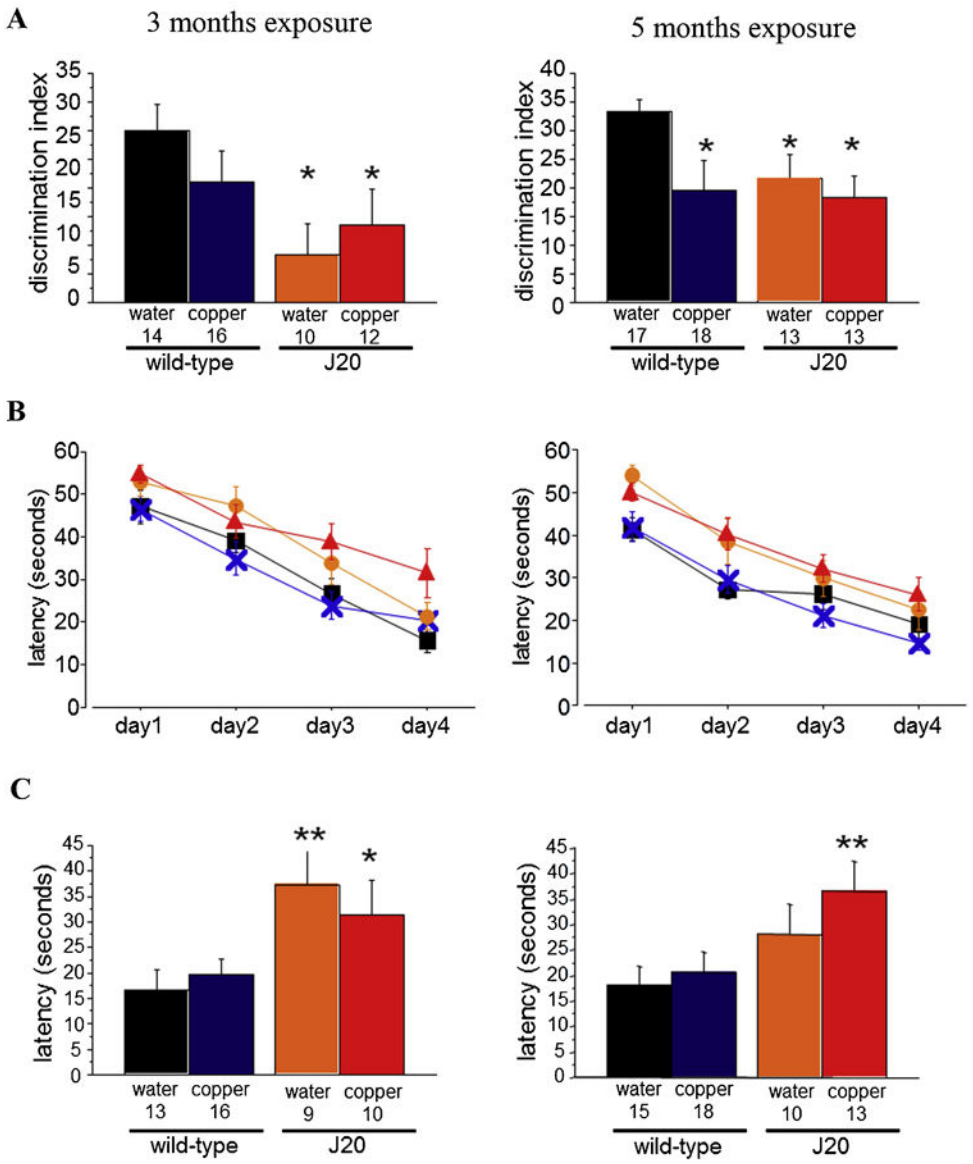

Figure 5. Chronic Cu exposure exacerbates spatial memory in mice.

(A) Object location discrimination index for mice exposed to Cu for 3 months (left), [genotype x treatment two-way ANOVA (genotype $F(1,48) = 6.82$ $P = 0.01$; treatment $F(1,48) = 0.11$ $P = 0.74$; interaction $F(1,48) = 1.58$ $P = 0.21$)], or 5 months (right), [genotype x treatment two-way ANOVA (genotype $F(1,57) = 2.48$ $P = 0.12$; treatment $F(1,57) = 4.23$ $P = 0.04$; interaction $F(1,57) = 1.57$ $P = 0.21$)]. **(B)** Latency to the platform during water maze training for mice exposed to Cu for 3 months (left) or 5 months (right). **(C)** Latency to the platform location in water maze test for mice exposed to Cu for 3 months (left), [genotype x treatment two-way ANOVA (genotype $F(1,44) = 10.74$ $P = 0.002$; treatment $F(1,44) = 0.08$ $P = 0.77$; interaction $F(1,44) = 0.82$ $P = 0.36$)], or 5 months (right), [genotype x treatment two-way ANOVA (genotype $F(1,52) = 7.29$ $P = 0.009$; treatment $F(1,52) = 1.34$ $P = 0.25$; interaction $F(1,52) = 0.35$ $P = 0.55$)]. Number of animals per group are indicated below each bar. Black = WT mice received water, blue = WT mice exposed to Cu, orange = J20 mice

received water, and red = J20 mice exposed to Cu. *$p < 0.05$, **$p < 0.01$ compared to the group of WT mice received water.

Table 1

Biological functions and diseases predicted by Ingenuity Pathway Analysis (IPA) to be activated based on significantly modulated translatomes (DEGs) between each pairwise comparisons. Color intensity indicates level of significance calculated as −log(p-value). Biological processes relate to cellular and immune responses and diseases involve inflammation, cognition and abnormalities are presented.

−log(p-value)	J20 (4 vs 6 mo)	WT vs J20 (4 mo)	WT vs J20 (6 mo)	WT/Cu (3 vs 5m exp)	WT Con vs Cu (3m exp)	WT Con vs Cu (5m exp)	J20/Cu (3 vs 5m exp)	J20 Con vs Cu (3m exp)	J20 Con vs Cu (5m exp)
Cellular Growth and Proliferation	3.20	0.00	4.06	7.92	2.75	4.29	2.30	0.00	3.09
Cellular Development	3.20	0.00	4.06	6.46	3.05	3.79	2.90	3.50	3.09
Cellular Function and Maintenance	3.60	0.00	3.42	6.16	2.75	3.88	2.90	1.83	2.40
Cell Death and Survival	4.42	0.00	3.26	7.58	3.05	3.86	1.66	0.00	3.09
Cellular Assembly and Organization	3.20	0.00	3.42	5.64	0.00	3.82	2.90	0.00	3.31
Cell Morphology	3.64	0.00	3.42	5.64	2.20	3.99	2.03	0.00	2.25
Cell Signaling	1.92	0.00	2.27	4.32	3.05	2.70	0.00	0.00	0.00
Cell-To-Cell Signaling and Interaction	4.35	0.00	3.09	5.40	2.49	3.33	2.50	2.49	2.40
Cell-mediated Immune Response	2.60	0.00	2.27	5.55	1.82	2.38	0.00	0.00	0.00
Cellular Movement	4.71	0.00	2.60	6.69	2.01	3.99	1.84	0.00	3.09
Immune Cell Trafficking	4.35	0.00	1.97	6.69	1.90	2.65	0.00	0.00	0.00
Antigen Presentation	3.20	0.00	0.00	3.65	0.00	0.00	2.20	0.00	0.00
Humoral Immune Response	2.69	0.00	1.79	6.01	0.00	3.33	2.50	0.00	0.00
Immunological Disease	3.20	0.00	2.60	5.71	3.05	4.29	0.00	1.84	0.00
Inflammatory Response	4.35	0.00	1.97	10.39	3.43	2.76	2.50	0.00	2.40
Inflammatory Disease	3.20	0.00	2.60	5.40	3.43	2.76	0.00	0.00	0.00
Infectious Diseases	3.20	0.00	3.18	5.45	3.84	2.32	0.00	0.00	0.00
Nervous System Development and Function	2.90	0.00	3.54	3.09	3.05	2.48	2.25	0.00	2.14
Neurological Disease	3.20	0.00	2.90	4.66	3.43	3.43	1.66	0.00	3.09
Behavior	1.43	0.00	3.44	0.00	2.75	2.34	0.00	0.00	1.72
Organismal Injury and Abnormalities	3.64	1.39	4.79	12.64	3.68	7.92	3.20	1.84	3.64
Cancer	3.20	1.39	4.79	12.64	3.14	7.92	2.90	1.84	3.64

Footnotes: J20: transgenic mouse model of AD; WT: wild-type mice; mo: month old; m: month; exp: exposed; Con: control or water-exposed; Cu: copper-exposed.